

Design and Development of Simvastatin Loaded Liposomes

Sujit Desai^{1,2*}, Arehalli Manjappa³, Preeti Khulbe¹

¹School of Pharmacy, Suresh Gyan Vihar University, Mahal Rd, Mahal, Jagatpura, Jaipur, Rajasthan, India

²Padmabhushan Krantiveer Dr. Nagnath Anna Nayakawadi College of Pharmacy, Walwa, Sangli, Maharashtra, India

³Department of Pharmaceutics, Vasantidevi Patil Institute of Pharmacy, Kodoli, Kolhapur Maharashtra, India

Received: 19th January, 2024; Revised: 14th March, 2024; Accepted: 09th May, 2024; Available Online: 25th June, 2024

ABSTRACT

Liposomes containing simvastatin were the focus of recent research. A process called thin film hydration was used to create simvastatin (SVN) liposomes. Method optimization was accomplished with the help of the BBD model. Drug content, vesicle size, surface shape, and *in-vitro* drug release were evaluated in the generated liposomes. There was no liposome that did not meet the criteria for appropriate drug content and mean vesicle size. Liposomes that did not combine and had a spherical or nearly spherical shape were seen in the surface morphology. The produced liposomes have demonstrated significant drug release. Liposomes loaded with SVN were successfully manufactured and tested.

Keywords: Simvastatin, *In-vitro* drug release, %Drug content, Liposomes

International Journal of Drug Delivery Technology (2024); DOI: 10.25258/ijddt.14.2.30

How to cite this article: Desai S, Manjappa A, Khulbe P. Design and Development of Simvastatin Loaded Liposomes. International Journal of Drug Delivery Technology. 2024;14(2):797-805.

Source of support: Nil.

Conflict of interest: None

INTRODUCTION

After intravenous administration, liposomal medications often demonstrate enhanced ADME and dynamics, which can widen the therapeutic frame, enhance efficacy, and mitigate toxicities associated with encapsulated drugs.^{1,2} Our previous research has shown that incorporating oils into liposomal membranes, alongside conventional components like phospholipids and cholesterol, offers several advantages.^{3,4} The aim of current study was to develop the efficacy of liposomal formulations of simvastatin. Simvastatin is a type of medication used to lower cholesterol levels, typically administered alongside a healthy diet, regular exercise, and weight loss efforts.^{5,6} It is also prescribed to reduce the risk of cardiovascular complications in high-risk individuals.^{7,8} Drug loading, average vesicle size, and *in-vitro* drug release kinetics were the main criteria used to evaluate the produced liposomes.^{9,10}

MATERIALS AND METHODS

We purchased the simvastatin (SVN) from Sigma Aldrich in Mumbai. Cholesterol was purchased from HiMedia Bangalore, while Lipoid GmbH of Germany supplied HSPC. The oil from soybeans was sourced from Molychem in India.¹¹

Preparation and Optimization of Liposomes

We used a thin film hydration approach to generate SVN-loaded liposomes¹² (Figure 1). A round bottom flask was used to combine HSPC, cholesterol, soybean oil, and the drug in a solvent system consisting of chloroform and methanol (2:1 ratio).^{13,14} The mixture was sonicated to ensure proper

dissolution of the excipients. Subsequently, the solution was heated in a water bath using a rotary evaporator at 60°C until a film formed. The film was then hydrated at 70°C until it dissolved completely. The hydrated film was sonicated using a probe sonicator with alternate heating cycles. This alternating heating and sonication process was repeated five times.^{15,16}

Experimental Design

The Box-Behnken design (BBD) model was utilized to optimize a process using Design-Expert 13 software. Three independent factors were identified in this multidimensional optimization procedure: HSPC (F1), cholesterol (F2), and soybean oil (F3) (Table 1). The responses measured were entrapment efficiency (R1) and particle size (R2).^{17,18}

Fourier-Transform Infrared Spectroscopy

FTIR analysis was used to assess potential drug-excipient interactions using the Cary-630 Agilent technology. In summary, the IR region was scanned using pure drugs SVN, CHOL, HSPC, soybean oil, and an equimolar (1 mM) physical mixture of SVN, HSPC, CHOL, and soybean oil. Concurrently, the liposomal formulations SVN-LIPO, as well as their coated dry powders, were characterized using the same procedure and conditions.¹⁹ The spectra were captured between wave numbers 4000 and 400 cm⁻¹.

Differential Scanning Calorimetry

Thermal properties and interactions between SVN and excipients were explored through differential scanning

*Author for Correspondence: sujitdesai37@gmail.com



Figure 1: Formulation batches of SVN-Loaded liposomes

Table 1: In BBD, variables, responses, coded levels, and limitations

Independent variables	High (+1)	Medium (0)	Low (-1)
X ₁ - HSPC (mg)	90.68	68.01	45.34
X ₂ - Cholesterol (mg)	92.02	51.75	11.48
X ₃ - Soyabean oil (mg)	56.69	31.88	7.07
Dependent variables (Factors)			
Y ₁ - Drug content (%) - Maximum			
Y ₂ - Vesicle size (nm) - Minimum			

calorimetry (DSC) analysis of both uncoated SVN and optimized coated SVN LPs (Lyophilized) using the SDT Q600 V20.9 Build 20 instrument. In order to create thermograms, samples with SVN and coated LPs were heated in a dry nitrogen environment from 0 to 500°C at a rate of 10° per minute. During the analysis, an empty metal pan was used as a reference.²⁰

X-ray Diffraction

X-ray diffraction (XRD) based physical examination was carried out to examine possible drug-carrier interactions. Diffraction patterns of both uncoated SVN and optimal coated SVN lyophilized (LPs) were captured by means of an X-ray diffractometer (Bruker D8 Advance) equipped with Cu-K α radiation ($\lambda = 1.54 \text{ \AA}$) operating at 40 kV and 50 mA. The diffraction angle (2θ) was scanned from 5 to 60° with raises of 0.02° at a rate of 1 s/step.²¹

Coating of SVN-loaded Liposomes

The necessary quantity of rhamnolipid for SVN was calculated and liquefied in 1-mL of methanol. Solutions were heated on a water bath at 60°C until a film formed. Subsequently, purified liposomes of each SVN were added to the respective films. The solutions were then heated in a water bath at 70°C using a hand-shaking method to ensure proper coating of the formulation.

Lyophilization of Coated Liposomes

During the lyophilization process, the lyophilizer was initially frozen for 1-hour, followed by a 20-minute warm-up period. Subsequently, a frozen sample containing vials was placed in the lyophilizer. For primary drying, a vacuum of 1.0 mbar was set for 2 hours. After the primary drying phase, the vacuum was

adjusted to 0.1 mbar for the remainder of the primary drying process. Once primary drying was completed, the vacuum was set to 0.001 mbar for secondary drying. Freeze drying of the coated formulations of simvastatin-loaded liposomes was conducted to obtain dry powder.

Drug content and Drug Entrapment Efficiency Determination

A UV-visible spectrophotometer (Agilent 1800) was used to evaluate the drug entrapment efficiency (DEE) and drug loading capacity (% DLC) of the LPs that were generated. As a whole, 0.1 mL of SVN-loaded LPs was mixed with 10 mL of methanol spun in a centrifuge, and the absorbance of the resulting supernatant was recorded at 235 nm.

Mean Particle Size and Zeta Potential

Produced LPs were centrifuged for 10 minutes at 10,000 rpm. Then, 0.1 mL of supernatant was collected from the centrifuged liposomes and diluted up to 10 mL using distilled water. The zeta potential and mean particle size of the formed LPs were measured using the Malvern ZS Zetasizer (Ver. 6.20, Malvern Instruments Ltd.). At a temperature of 20°C, each measurement was repeated three times.

In-vitro Drug Release Study

In-vitro dissolution release study of SVN was conducted using the dialysis bag technique and pure API solutions. A USP type II (paddle) device was employed for dissolution. Initially, 100 mL of dissolving liquid containing phosphate buffer (pH 7.4) was added to the vessel. To provide more detail, dialysis tubes with a molecular weight cutoff of 12000 were filled with SVN (5 mg) and SVN-loaded liposomes (equivalent to 5 mg). These dialysis bags were securely tied to paddles and immersed in vessels containing the dissolution medium. The test environment was maintained at 37°C throughout the experiment, with the paddle's rotation speed set to 100 rpm.

About 3 mL of the release medium was removed and replaced with a volume of new buffer medium at predetermined intervals (0.5, 1, 2, 4, 6, 8, 12, 24, 48, and 72 hours). The next step was to use a 235 nm UV-spectrophotometer to examine each sample. Every sample went through this procedure three times. The proportion of total drug release was calculated by plotting the release behavior against time.

Stability Study of Liposomes

For a duration of one month, liposomal formulations were kept at temperatures ranging from 2 to 8°C and at room temperature. A cryoprotectant of 5% sucrose was included in these formulations. After 15 and 30 days of storage, the formulations were tested using UV-visible spectroscopic analysis for entrapment efficiency (EE) and drug loading efficiency (DLE).

The supernatant was obtained after centrifuging 1-mL of the formulation to evaluate the EE and DLE. Next, 1 mL of methanol was added to the supernatant, and then it was sonicated for 10 minutes to make sure it was completely dissolved. Using ultraviolet-visible spectroscopy, we found that the supernatant contained SVN.^{22,23}

RESULTS AND DISCUSSION

FTIR Analysis

To explore possible drug-excipient interactions amongst SVN, cholesterol, soybean oil, di-rhamnolipid, and HSPC, infrared spectroscopy investigations were carried out (Figure 2, and Table 2). None of the medicine's characteristic peaks were

Table 2: FTIR values of formulations

IR values of functional groups of SVN				
Sr. No.	Functional group	Peak (cm^{-1}) (Standard)	Peak (cm^{-1}) (Observed)	Indication (Vibrations)
1	O-H	3500–3200	3284	Stretching
2.	N-H	3000–2850	2923	Stretching
3.	P=O	1275–1000	1260	Bending
4.	C-H	2000–1650	1655	Stretching
IR values of functional groups of SVN-loaded LPs				
1.	O-H	3500–3200	3282	Stretching
2.	N-H	3000–2850	2919	Stretching
3.	C=O	1750–1735	1741	Stretching
4.	P=O	1275–1000	1039	Bending

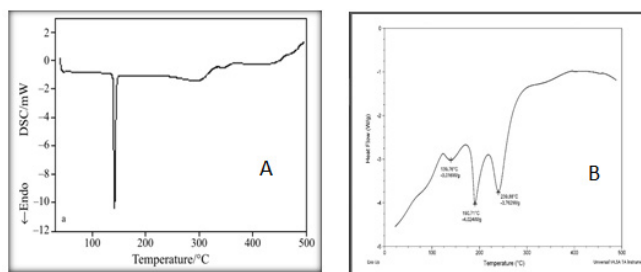


Figure 3: DSC of A) SVN & B) SVN-loaded LPs

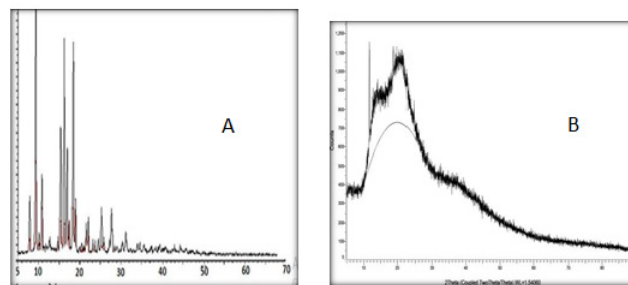


Figure 4: XRD of A) SVN & B) SVN-loaded LPs

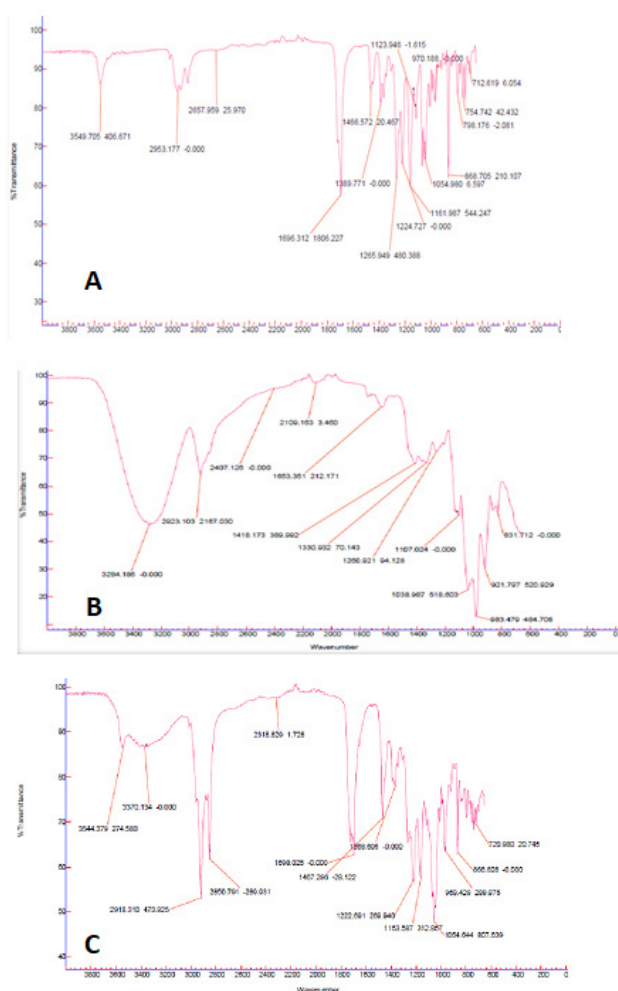


Figure 2: FTIR of A) SVN, B) Physical mixture & C) SVN loaded LPs

missing from the data, suggesting that the drug and excipients did not interact chemically. It appears that the medication remains stable within its liposomal structure.

DSC Analysis

Figure 3 displays the DSC thermograms of pure SVN alongside coated powders under a dry, inert nitrogen atmosphere. In the DSC thermogram, a peak corresponding to SVN is observed at 135 to 138°C. Additionally, an endothermic peak at 139.75°C is evident in the DSC thermogram of SVN and formulation excipients. Interestingly, the melting temperature peak of SVN decreased when excipients were enclosed in coated SVN LPs, indicating a disorganized crystallinity of molecular distribution within the polymer matrix.

XRD Analysis

Figure 4 presents the XRD patterns of standard SVN and coated lyophilized SVN. In the XRD pattern of plain SVN, distinct high-energy diffraction peaks are observed, indicating its crystalline behavior. However, the XRD patterns of coated lyophilized SVN-LPs show typical high-energy diffraction patterns, suggesting that the formulation is amorphous in nature.

Experimental design

The liposomal formulation's properties were optimized using a three-factor, three-level Box-Behnken design (BBD). For this analysis, we used the three variables. The thin film hydration approach was used to make seventeen preparation batches of SVN-liposomes. Then, in order to do statistical analysis, the gathered data on response variables were reviewed for important information. The following equation represents the derived quadratic polynomial model from the variables and responses:

$$Y = \beta_0 + \beta_1A + \beta_2B + \beta_3C + \beta_4AB + \beta_5AC + \beta_6BC + \beta_7A^2 + \beta_8B^2 + \beta_9C^2$$

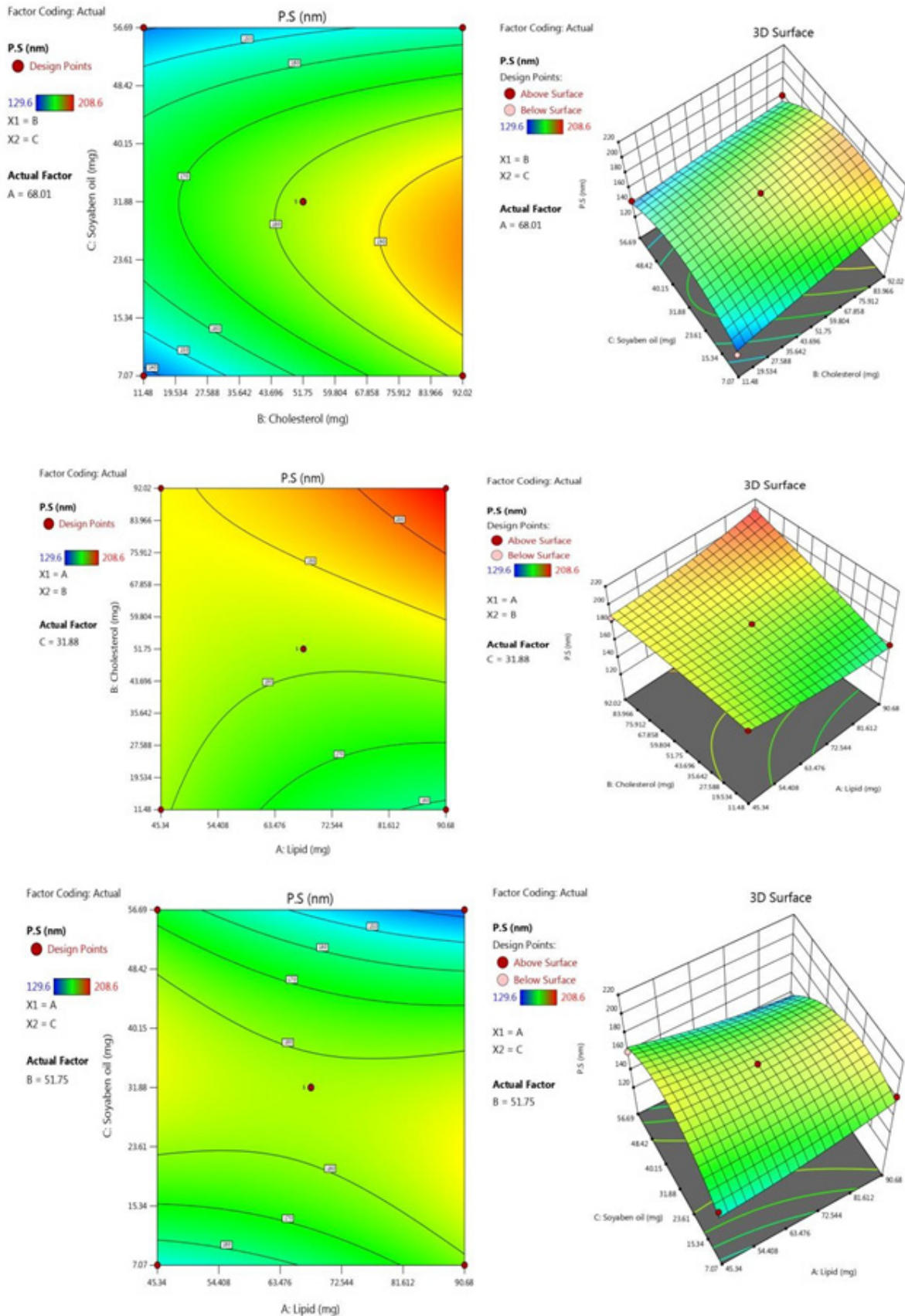


Figure 5: 2D & 3D plots showing the effect of AB, AC & BC on the particle size (Y1) of SVN

Where Y represents measured response variables (e.g., particle size, %entrapment efficiency) associated with each combination of different factor levels, as observed, the independent variables are denoted by the codes A, B, and C.

The quadratic model was found to be significant ($p < 0.05$) for the design according to the ANOVA results. The produced polynomials were considerably well-fit at $p < 0.05$, as evidenced by the corrected R^2 values of 0.9449 for particle size and 0.9119 for %entrapment efficiency.

The effective independent variables for each response were observed and determined using two-dimensional (2D) and three-dimensional (3D) graphs that were generated after the analysis of Design of Experiment (DoE) data. By analyzing the developed formulations, these graphs shed light on the impact of each variable on each response. Figures show the results of the meticulous examination that was carried out in order to determine the direct effects and interactions between variables. This information was crucial for the experimental model selection process.

Influence of Input Variables

This regression coefficient equation expresses the total influence of different factors on particle size (PS). The magnitude of the independent variables' synergistic and antagonistic impacts on the response are represented by the positive and negative signs of the regression coefficients in the equation, respectively. The 2D and 3D response surfaces showing the input variable effects on PS are shown in Figure 5. The chosen variables were shown to have a substantial impact on PS.

A significant connection between experimental and anticipated findings was indicated by the quadratic model for PS, which had a p -value less than 0.05 and a difference of less

than 0.2 between the adjusted R^2 (0.9119) and predicted R^2 (0.7410). Furthermore, there were sufficient signals to traverse the design space, as determined by the signal-to-noise ratio ($14.251 > 4$), which is an indicator of sufficient precision.

Based on the response graph for PS, it appears that a higher lipid (HSPC):cholesterol ratio causes PS to rise, whereas lower ratios of CHOL:soybean oil and Lipid:soybean oil show declining PS behavior.

$$PS = +182.40i + 0.6625A + 14.71B - 6.63C + 10.85AB - 13.83AC - 7.58BC + 3.67A^2 - 1.53B^2 - 27.95C^2$$

In the proposed quadratic model, the impact of certain parameters on %entrapment efficiency (%EE) is summarized by the polynomial equation. The model was statistically significant, with a high F-value of 14.33, suggesting a low margin of error. Its agreement is further supported by the model's strong R^2 score (0.9573). The selected model is suitable for further exploration of the design space because the difference between the anticipated R^2 (0.8874) and modified R^2 (0.9449) is very small, less than 0.2.

Figure 6 shows contour plots for %EE in two and three dimensions. A high lipid:cholesterol ratio can be reached with a low %EE, as seen clearly in the graphs. The same holds true for soybean oil: lipid and CHOL: soybean oil ratios; low %EE is preferred. Based on these findings, it appears that these factors impact the %EE response.

$$\%EE = +32.20i + 1.54A + 4.36B + 4.69C - 1.91AB - 4.59AC - 1.30BC + 10.84A^2 + 8.25B^2 + 4.05C^2$$

Coating of SVN Liposomes & Lyophilization

The coating of SVN-loaded and blank liposomes was accomplished using di-rhamnolipid. Di-rhamnolipid, a microbial biosurfactant, was employed as a coating agent to enhance the microbial activity of the drug (Figures 7 and 8).

Table 3: Design matrix of SVN-loaded liposomes as per Box-Behnken design

Batches	Factor 1 lipid (mg)	Factor 2 cholesterol (mg)	Factor 3 soyabean oil (mg)	Response 1 %EE (%)	Response 2 particle size (nm)
1.	45.34	11.48	31.88	25.7 ± 3.55	182.2 ± 4.47
2.	90.68	92.02	31.88	50.6 ± 5.06	208.6 ± 3.68
3.	68.01	51.75	31.88	39.9 ± 3.19	182.4 ± 4.72
4.	45.34	51.75	56.69	27.3 ± 3.51	161.1 ± 4.24
5.	90.68	11.48	31.88	44.3 ± 3.30	161.1 ± 3.35
6.	68.01	92.02	7.07	43.45 ± 2.96	177.8 ± 3.55
7.	90.68	51.75	7.07	52.2 ± 4.31	182.8 ± 1.59
8.	68.01	92.02	56.69	52.85 ± 4.10	261.0 ± 4.93
9.	68.01	11.48	7.07	33.55 ± 2.95	129.6 ± 4.45
10.	45.34	51.75	7.07	32.2 ± 5.12	158.4 ± 3.93
11.	68.01	11.48	56.69	48.15 ± 4.28	143.2 ± 2.60
12.	90.68	51.75	56.69	52.8 ± 5.37	130.2 ± 4.11
13.	45.34	92.02	31.88	62.1 ± 2.40	186.3 ± 2.82
14.	68.01	51.75	31.88	39.9 ± 3.19	182.4 ± 4.72
15.	90.68	51.75	7.07	52.2 ± 4.31	182.8 ± 1.59
16.	68.01	51.75	31.88	39.9 ± 3.19	182.4 ± 4.72
17.	68.01	51.75	31.88	39.9 ± 3.19	182.4 ± 4.72

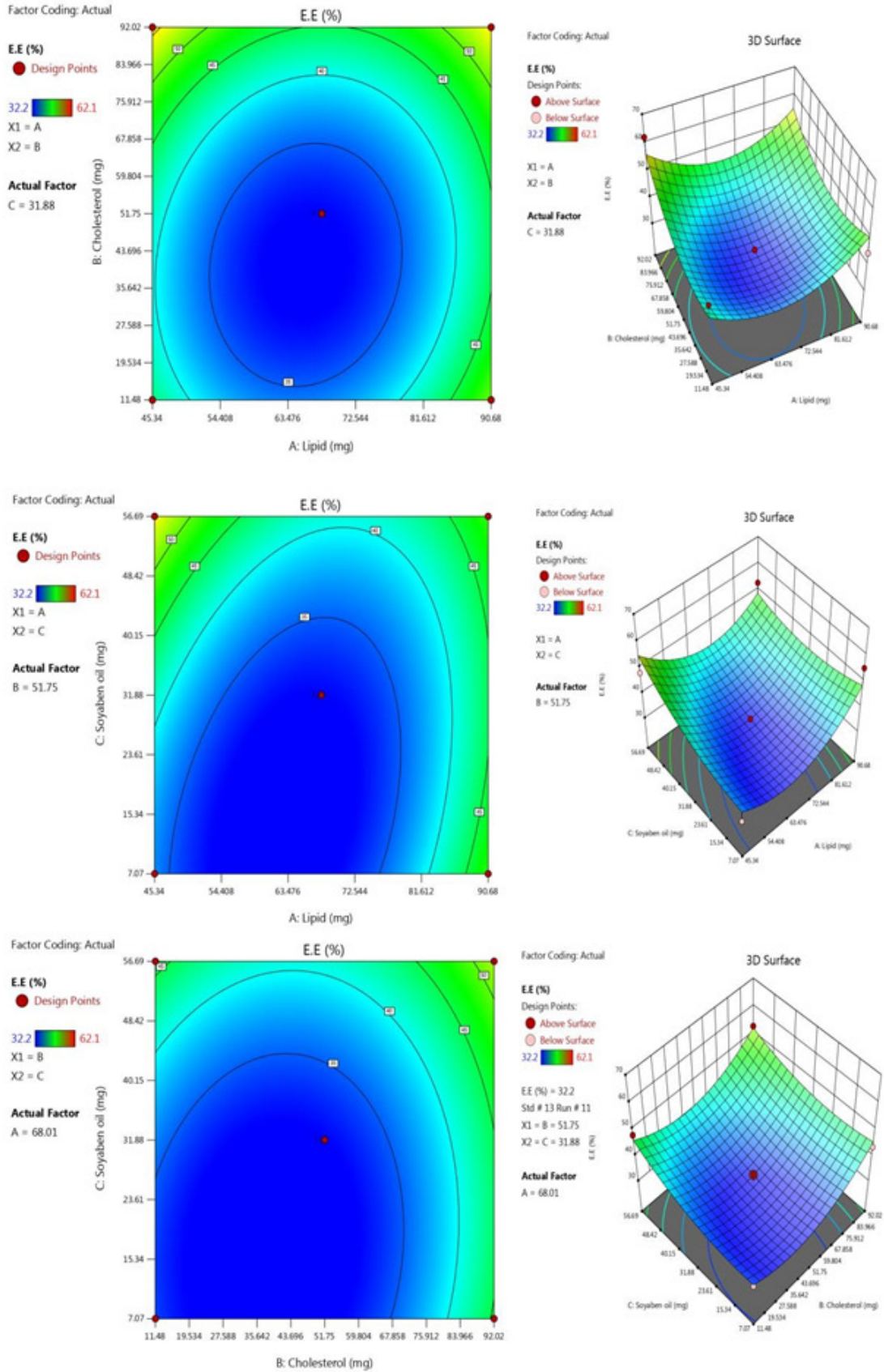


Figure 6: 2D & 3D plots showing effect of AB, AC & BC on the entrapment efficiency (Y2) of SVN



Figure 7: Coated formulations of blank liposomes, simvastatin liposomes



Figure 8: Freeze-dried coated powders of blank liposomes & simvastatin liposomes

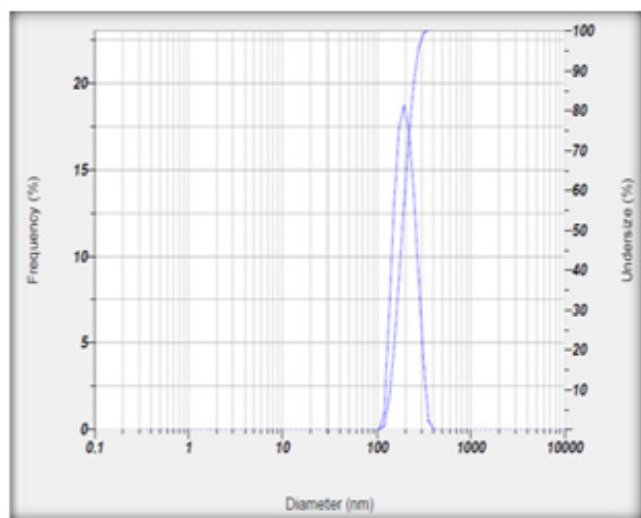


Figure 9: Particle size of optimized batch of SVN-loaded LPs

Characterization of SVN liposomes

%Entrapment efficiency

Table 3 summarizes the percentage entrapment efficiency of simvastatin into liposomes for all seventeen batches. Each batch demonstrates entrapment efficiency within a certain range. For instance, SVN batch-12 exhibited an entrapment efficiency of $52.8 \pm 5.37\%$. It's important to note that higher entrapment efficiency indicates greater drug loading within the liposomes.

Particle size of SVN-loaded liposomes

The particle size of optimized SVN-loaded liposomes was found to be in the nanometer range, as depicted in Figure 9, Table 4.

Zeta potential of SVN-loaded liposomes

Figure 10 illustrates the zeta potential of SVN-loaded liposomes. The liposomes exhibited a negative zeta potential (-mV), indicating their anionic nature. Previous research

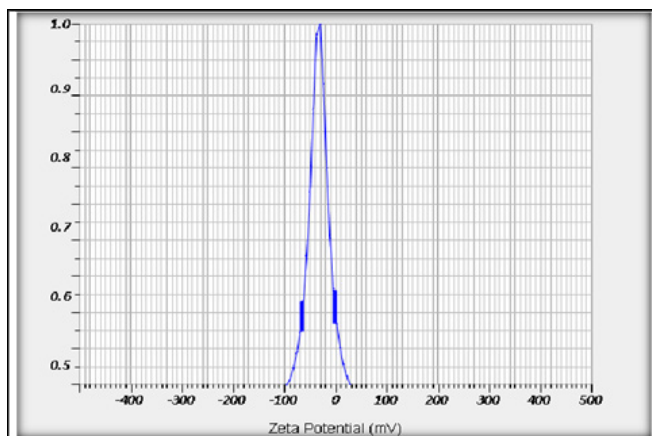


Figure 10: Zeta potential of SV-loaded LP's

Table 4: Particle size and zeta potential of optimized SVN-loaded liposomes

Batch	Particle size (nm)	Zeta potential (mV)
Optimized SVN Batch 12	130.2	-33.3

Table 5: Drug release of SVN & optimized batch of SVN

Time	%Drug release of SVN LPs	%Drug release of plain simvastatin
0.5	11.0812 ± 2.39	21.6576 ± 2.97
1	31.3604 ± 1.34	43.7079 ± 4.71
2	36.0974 ± 3.50	50.9607 ± 6.47
4	40.1921 ± 3.35	59.6319 ± 4.73
6	42.5132 ± 5.90	62.5977 ± 4.92
8	47.8659 ± 7.41	70.1425 ± 3.43
12	55.8582 ± 4.48	76.9768 ± 4.13
24	65.7556 ± 3.90	88.4533 ± 2.54
48	82.8743 ± 4.06	97.9613 ± 2.30

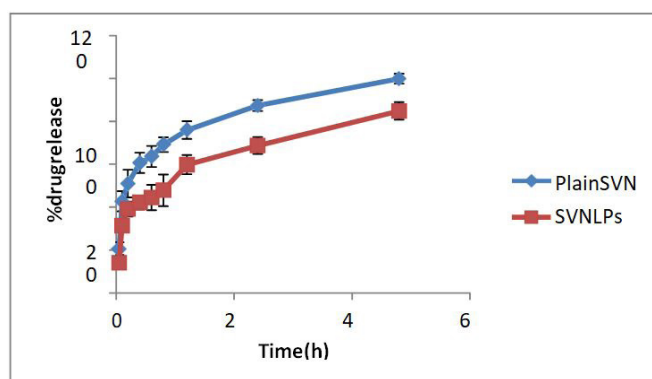


Figure 11: *In-vitro* drug release study of optimized SVN Batch 12

suggests that poly-anions possess greater bio-adhesive strength compared to poly-cations. The negative zeta potential of liposomes indicates their stability.

Drug Release Study

The drug release study is reported in Table 5, Figure 11.

Table 6: Stability study of LPs

Batch	%EE at day 0	%EE after 1 month	%EE after 3 months	%EE after 6 months
SVN 12	52.8 ± 5.37	48.4 ± 4.78	45.54 ± 5.46	40.23 ± 6.71

Stability study

The prepared SVN formulation exhibited stable results even after 1, 3, and 6 months. The stability of the formulation was confirmed, and the results are presented in Table 6. The %entrapment efficiency (%EE) of SVN was calculated using UV-visible spectroscopy at 235 nm.

CONCLUSION

The recent research focused on liposomes that contained simvastatin. Simvastatin (SVN) liposomes were created using a technique termed thin film hydration. The BBD model was used to optimize the method. The liposomes were assessed for drug content, vesicle size, surface form, and *in-vitro* drug release. All liposomes met the criterion for appropriate medication content and mean vesicle size. The surface morphology revealed the presence of liposomes that exhibited a spherical or nearly spherical form and did not aggregate. The liposomes that were created have shown a substantial release of drugs. SVN-loaded liposomes were effectively produced and evaluated.

REFERENCES

- Luo D, Carter KA, Molins EA, Straubinger NL, Geng J, Shao S, Jusko WJ, Straubinger RM, Lovell JF. Pharmacokinetics and pharmacodynamics of liposomal chemophototherapy with short drug-light intervals. *Journal of controlled release*. 2019 Mar 10;297:39-47. Available from: 10.1016/j.jconrel.2019.01.030
- Lindsey BA, Markel JE, Kleinerman ES. Osteosarcoma overview. *Rheumatology and therapy*. 2017 Jun; 4:25-43. Available from: 10.1007/s40744-016-0050-2
- Kumbhar P, Kole K, Khadake V, Marale P, Manjappa A, Nadaf S, Jadhav R, Patil A, Singh SK, Dua K, Jha NK. Nanoparticulate drugs and vaccines: breakthroughs and bottlenecks of repurposing in breast cancer. *Journal of Controlled Release*. 2022 Sep 1;349:812-830. Available from: 10.1016/j.jconrel.2022.07.039
- Deshantri AK, Fens MH, Ruiter RW, Metselaar JM, Storm G, Mandhane SN, Graat GH, Lentjes EG, Yuan H, de Bruijn JD, Mutis T. Complete tumor regression by liposomal bortezomib in a humanized mouse model of multiple myeloma. *HemaSphere*. 2020 Oct 1;4(5):e463. Available from: 10.1097/HS9.0000000000000463
- Sambamoorthy U, Manjappa AS, Eswara BR, Sanapala AK, Nagadeepthi N. Vitamin E oil incorporated liposomal melphalan and simvastatin: approach to obtain improved physicochemical characteristics of hydrolysable melphalan and anticancer activity in combination with simvastatin against multiple myeloma. *AAPS PharmSciTech*. 2022 Jan;23:1-6. Available from: 10.1208/s12249-021-02177-6
- Peram MR, Jalalpure S, Kumbar V, Patil S, Joshi S, Bhat K, Diwan P. Factorial design-based curcumin ethosomalnanocarriers for the skin cancer delivery: in-vitro evaluation. *Journal of liposome research*. 2019 Jul 3;29(3):291-311. Available from: 10.1080/08982104.2018.1556292
- Galatage ST, Manjappa AS, Bhagwat DA, Trivedi R, Salawi A, Sabei FY, Alsalthi A. Oral self-nanoemulsifying drug delivery systems for enhancing bioavailability and anticancer potential of fosfestrol: In-vitro and in vivo characterization. *European Journal of Pharmaceutics and Biopharmaceutics*. 2023 Dec 1; 193:28-43. Available from: 10.1016/j.ejpb.2023.10.013
- Ju C, Zhang C. Preparation and Characterization of pH Sensitive Drug Liposomes. *Liposome-Based Drug Delivery Systems*. 2021:385-408. Available from: https://doi.org/10.1007/978-3-662-49320-5_14
- Mast MP, Modh H, Knoll J, Fecioru E, Wacker MG. An Update to Dialysis-Based Drug Release Testing—Data Analysis and Validation Using the Pharma Test Dispersion Releaser. *Pharmaceutics*. 2021 Nov 25;13(12):2007. Available from: 10.3390/pharmaceutics13122007
- Yadav P, Rastogi V, Verma A. Application of Box–Behnken design and desirability function in the development and optimization of self-nanoemulsifying drug delivery system for enhanced dissolution of ezetimibe. *Future Journal of Pharmaceutical Sciences*. 2020 Dec;6(1):1-20. Available from: <https://doi.org/10.1186/s43094-020-00023-3>
- Singh V, Haque S, Niwas R, Srivastava A, Pasupuleti M, Tripathi C. Strategies for fermentation medium optimization: an in-depth review. *Frontiers in microbiology*. 2017 Jan 6;7:2087. Available from: 10.3389/fmicb.2016.02087
- Unnisa A, Chettupalli AK, Alazragi RS, Alelwani W, Bannunah AM, Barnawi J, Amarachinta PR, Jandrajupalli SB, Elamine BA, Mohamed OA, Hussain T. Nanostructured Lipid Carriers to Enhance the Bioavailability and Solubility of Ranolazine: Statistical Optimization and Pharmacological Evaluations. *Pharmaceutics*. 2023 Aug 14;16(8):1151. Available from: 10.3390/ph16081151
- Hirabayashi H, Takahashi T, Fujisaki J, Masunaga T, Sato S, Hiroi J, Tokunaga Y, Kimura S, Hata T. Bone-specific delivery and sustained release of diclofenac, a non-steroidal anti-inflammatory drug, via bisphosphonic prodrug based on the Osteotropic Drug Delivery System (ODDS). *Journal of controlled release*. 2001 Jan 29;70(1-2):183-191. Available from: [https://doi.org/10.1016/s0168-3659\(00\)00355-2](https://doi.org/10.1016/s0168-3659(00)00355-2)
- Jing C, Li B, Tan H, Zhang C, Liang H, Na H, Chen S, Liu C, Zhao L. Alendronate-decorated nanoparticles as bone-targeted alendronate carriers for potential osteoporosis treatment. *ACS Applied Bio Materials*. 2021 May 19;4(6):4907-4916. Available from: 10.1021/acsabm.1c00199
- Olusanya TO, Haj Ahmad RR, Ibegbu DM, Smith JR, Elkordy AA. Liposomal drug delivery systems and anticancer drugs. *Molecules*. 2018 Apr 14;23(4):907. Available from: 10.3390/molecules23040907
- Nunes SS, Miranda SE, de Oliveira Silva J, Fernandes RS, de Alcântara Lemos J, de Aguiar Ferreira C, Townsend DM, Cassali GD, Oliveira MC, de Barros AL. pH-responsive and folate-coated liposomes encapsulating irinotecan as an alternative to improve efficacy of colorectal cancer treatment. *Biomedicine & Pharmacotherapy*. 2021 Dec 1; 144:112317. Available from: <https://doi.org/10.1016/j.biopha.2021.112317>
- Mane V, Killedar S, More H, Nadaf S, Salunkhe S, Tare H. Novel Phytosomal Formulation of Emblica officinalis Extracts with Its In Vivo Nootropic Potential in Rats: Optimization and Development by Box-Behnken Design. *Journal of Chemistry*. 2024;2024(1):6644815. Available from: <http://dx.doi.org/10.1155/2024/6644815>
- Patil K, Narkhede S, Nemade M, Rane S, Chaudhari R,

- Dhobale G, Tare H. A Validated Sensitive Stability Indicating HPLC Method for the Determination of Etoricoxib in Bulk and Formulation. *International Journal of Pharmaceutical Quality Assurance*. 2023;14(2):352-357. Available from: <http://dx.doi.org/10.25258/ijpqa.14.2.19>
19. Mane V, Killedar S, More H, Tare H. Preclinical study on camellia sinensis extract-loaded nanophytosomes for enhancement of memory-boosting activity: optimization by central composite design. *Future Journal of Pharmaceutical Sciences*. 2024 May 1;10(1):66. Available from: DOI<https://doi.org/10.1186/s43094-024-00639-9>
20. Chattar H, Pimple B, Kuchekar M, Tare H, Wagh V, Kachave R. Comparative antifungal potential of six formulated herbal shampoos against *Candida albicans* causing Seborrheic dermatitis. *Microbial Biosystems*. 2024 Jun 1;9(1):17-26. Available from: <https://doi.org/10.21608/mb.2024.353426>
21. Kharate V, Kuchekar M, Harde M, Pimple B, Patole V, Salunkhe M, Wadgave P, Bhise M, Gaikwad A, Tare H. Development of Validated Stability Indicating HPTLC Method for Estimation of Febuxostat in Bulk and Tablet Dosage Form by Using QBD Approach. *International Journal of Drug Delivery Technology*. 2023;13(2):542-550. Available from: <http://dx.doi.org/10.25258/ijddt.13.2.14>
22. Mane VB, Killedar SG, More HN, Tare HL. Evaluation of acute oral toxicity of the *Embllica officinalis* Phytosome Formulation in Wistar Rats. *International Journal of Drug Delivery Technology*. 2022;12(4):1566-1570. Available from: 10.25258/ijddt.12.4.14
23. Ahmad S, Shaikh TJ, Patil J, Meher A, Chumbhale D, Tare H. Osmotic Release Oral Tablet Formulation, Development, and Evaluation of an Anti-epileptic Drug. *International Journal of Drug Delivery Technology*. 2023;13(1):305-312. Available from:10.25258/ijddt.13.1.50